

UC Davis

UC Davis Previously Published Works

Title

DLC2 modulates angiogenic responses in vascular endothelial cells by regulating cell attachment and migration

Permalink

<https://escholarship.org/uc/item/811402fb>

Journal

Oncogene, 29(20)

ISSN

0950-9232

Authors

Lin, Y
Chen, N-T
Shih, Y-P
[et al.](#)

Publication Date

2010-05-20

DOI

10.1038/onc.2010.54

Peer reviewed



Published in final edited form as:

Oncogene. 2010 May 20; 29(20): 3010–3016. doi:10.1038/onc.2010.54.

DLC2 modulates angiogenic responses in vascular endothelial cells by regulating cell attachment and migration

Yuan Lin^{1,2}, Nein-Tsu Chen¹, Yi-Ping Shih¹, Yi-Chun Liao¹, Ling Xue², and Su Hao Lo^{1,*}

¹Department of Biochemistry and Molecular Medicine University of California-Davis, Sacramento, CA 95817. USA

²Department of Pathology, First Affiliated Hospital, Sun Yat-Sen University Guangzhou, Guangdong 510080, China

Abstract

Deleted in Liver Cancer 1 (DLC1) is a RhoGAP-containing tumor suppressor that associates with various types of cancer. Although DLC2 shares a similar domain structure with that of DLC1, the function of DLC2 is not well characterized. Here, we describe the expression and ablation of DLC2 in mice using a reporter-knockout approach. DLC2 is expressed in several tissues and in endothelial cells (ECs) of blood vessels. Although ECs and blood vessels show no histological abnormalities and mice appear overall healthy, DLC2 mutant mice display enhanced angiogenic responses induced by matrigel and by tumor cells. Silencing of DLC2 in human ECs has reduced cell attachment, increased migration, and tube formation. These changes are rescued by silencing of RhoA, suggesting that the process is RhoA pathway dependent. These results indicate that DLC2 is not required for mouse development and normal vessel formation, but may protect mouse from unwanted angiogenesis induced by for example tumor cells.

Keywords

DLC2; RhoGAP; tumor suppressor; angiogenesis

Introduction

Deleted in liver cancer (DLC) is a group of three genes that are highly related to each other based on their amino acid sequences (Liao & Lo, 2008). They all contain the SAM (sterile alpha motif), RhoGAP (RhoGTPase activation protein), and START (steroidogenic acute regulatory (StAR)-related lipid transfer) domains, and localize to focal adhesion sites. DLC1 was isolated as a candidate tumor suppressor for liver cancer (Yuan et al., 1998). Further studies have detected down-regulation of DLC1 in various types of cancers. Genomic

Users may view, print, copy, download and text and data- mine the content in such documents, for the purposes of academic research, subject always to the full Conditions of use: http://www.nature.com/authors/editorial_policies/license.html#terms

*Corresponding author Su Hao Lo, Department of Biochemistry and Molecular Medicine, University of California-Davis, 4635 Second Ave. Room 3002, Sacramento, CA 95817. T:916-734-3656, F:916-734-5750. shlo@ucdavis.edu.

No potential conflicts of interest

Conflict of interest The authors declare no conflict of interest.

deletion and promoter hypermethylation are two main causes of DLC1 down-regulation in cancer patients (Durkin et al., 2007b). Mutations that lead to early translational termination and functional alteration of DLC1 protein have also been identified (Liao et al., 2008). DLC1 is known to regulate cell shape, attachment, migration, proliferation and cell survival (Durkin et al., 2007b; Liao & Lo, 2008). Re-expression of DLC1 in DLC1 null cancer cell lines efficiently suppresses cancer cell growth. The tumor cell suppression activity is highly reliant on DLC1's RhoGAP domain and focal adhesion localization (Liao et al., 2007; Qian et al., 2007). These findings strongly suggest that DLC1 is a bona fide tumor suppressor.

DLC2 (also called STARD13) protein shares the same domain structure with DLC1. It is also under-expressed in some types of cancer and suppresses tumor cell growth by inhibition of RhoA activity through its RhoGAP domain (Ching et al., 2003; Leung et al., 2005; Ullmannova & Popescu, 2006). Significant correlations between under-expression of DLC2 and cell differentiation as well as overexpression of RhoA in hepatocellular carcinoma have been reported (Xiaorong et al., 2008). Patients with DLC2-negative expression showed a significantly poorer prognosis than those with DLC2-positive hepatocellular carcinoma (Xiaorong et al., 2008). However, the overall expression pattern of DLC2 and its in vivo function are largely unknown.

In this report, we describe the expression pattern of DLC2, the effect of DLC2 deletion in mice, the role of DLC2 in endothelial cells, and its function in angiogenesis.

Results

Generation of DLC2 reporter knockout mice

To investigate the in vivo function of DLC2, we generated DLC2 knockout (KO) mice by using a DLC2 targeted ES cell clone from the Knockout Mouse Project Repository. The targeting vector was constructed (figure 1A) using the promoterless targeting cassette with the En2 splice acceptor/ β -galactosidase/Neo/Poly-A sequences flanked by two FRT sites followed by the mouse DLC2 exon 3 flanked by two loxP sites for the generation of a “knockout-first allele” (Testa et al., 2004). The engineered β -galactosidase is expressed only under the endogenous DLC2 promoter and simultaneously disrupts the expression of DLC2. This targeting strategy allows us to produce reporter knockouts, and if necessary conditional knockouts and null alleles by exposure to site-specific recombinases Cre and Flp. Only reporter knockouts are described in this report. The mouse genotypes were determined by PCR assay (figure 1B). To confirm the lack of DLC2 protein expression, tissue lysates from wild type (WT) and homozygous mice were immunoprecipitated and immunoblotted with anti-DLC2 or anti- β -galactosidase antibodies (figure 1C). The lack of DLC2 in the homozygous lung, liver, kidney and heart demonstrated the interruption of DLC2 expression in the mutant mice. The presence of β -galactosidase in the KO tissue samples further confirmed the replacement of DLC2 by the reporter.

DLC2 overall expression pattern in a mouse

Although we have developed antibodies against DLC2 suitable for immunoprecipitation and immunoblot assays (figure 1C), the antibodies do not appear to detect DLC2 by

immunohistochemistry (IHC) staining. In order to analyze DLC2 expression pattern, we utilized the reporter system of DLC2 mutant mice with X-gal staining (figure 2A). Very intense X-gal blue staining was detected in alveolar epithelial cells of lung, hepatocytes of liver, cardiac myocytes in heart, and ependymal cells of brain. In stomach, the stained cells were found in muscularis, lamina propria, but not in epithelium. In kidney, the staining was strong in renal tubules of papilla and medulla regions, but was dispersed in the cortex area except the medullary ray. In testis, the stained cells were in the center of the seminiferous tubule while the peripheral cells had no staining. In ovary, staining was observed in oocytes. No staining in granulosa cells of follicles but strong staining in all the granular lutein cells of corpus luteum was detected (not shown). Staining was also observed in islets in pancreas, epithelium of prostate, pigmented epithelium and ciliary processed of the eye. Although there was X-gal positive staining in thymus, spleen, skeletal muscle, small intestine, colon, and other tissues, the staining patterns were similar to the blood vessels. To confirm this, umbilical vessels, stomach, and skeletal muscle were sectioned for CD31 (a surface marker for endothelial cells) and X-gal staining (figure 2B). The results demonstrated that the X-gal staining was highly concentrated at endothelial cells. Tissue samples shown in figure 2 were from DLC2 homozygous mice. Nonetheless, DLC2 heterozygous mice display the same X-gal staining pattern (not shown).

Loss of DLC2 promotes angiogenesis

Despite DLC2 being expressed in various tissues, we failed to observe histological abnormality in DLC2 KO mice (as shown in figure 2) and mice appeared normal and healthy, indicating that DLC2 is not required for embryo development and mouse survival. In addition, the microvascular density and morphology in stomach, skeletal muscle, brain were examined and no difference between WT and KO mice was detected (figure 2; data not shown). The fact that DLC2 is highly concentrated in endothelial cells but does not produce an overt phenotype in mice has prompted us to challenge these mice with matrigel to assess the role of DLC2 during angiogenesis. Matrigel (growth factors reduced) was injected subcutaneously into WT and KO mice to induce neovascularization and formed matrigel plugs were removed and analyzed 4 day later. The matrigel plugs from the KO mice appeared bloodier and had a higher hemoglobin concentration than the WT (figure 3A). IHC staining also confirmed a significantly higher population of CD31 positive cells in plugs from KO. To further examine DLC2's function in vessel formation, mouse aorta sections were grown in a 3D matrigel culture to observe EC sprouting. Consistent with in vivo matrigel plug results, we detected significantly increased ex vivo sprouting in DLC2 KO samples (figure 3B). These data suggest that DLC2 may modulate angiogenic responses of endothelial cells.

Lack of DLC2 enhances angiogenesis induced by tumor cells but not by wound

As loss of DLC2 promotes angiogenesis in Matrigel plug assay, we further analyzed angiogenesis induced by wound in WT mice and DLC2 KO mice. The rate of skin wound healing showed no apparent difference between these two groups of mice. The vascular density was evaluated by CD31 IHC staining 7 days after wound in order to quantify wound-induced angiogenesis. The result showed similar microvascular densities in the granulation tissues of DLC2 KO mice compared to the WT mice (figure 4A). We further

analyzed whether loss of DLC2 could promote angiogenesis induced by tumor cells. B16 murine melanoma tumor cells were implanted into the dorsal skin of WT and DLC2 KO mice. After 11 days, the mean size of tumors implanted in DLC2 KO mice was significantly larger than that in WT mice (figure 4B). In addition, the microvascular densities in tumors were significantly higher in KO than WT mice (figure 4B).

DLC2 regulates endothelial cell attachment and migration through a RhoA dependent pathway

To analyze the role of DLC2 in endothelial cells and the molecular mechanism involved, we have applied the siRNA approach. Silencing of DLC2 in HUVECs (human umbilical vein endothelial cells) significantly reduced cell attachment and promoted cell migration (figure 5). In addition, down-regulation of DLC2 also enhanced tube formation of HUVEC on matrigel. These in vitro results are consistent with our in vivo findings and support the idea that DLC2 negatively regulates angiogenesis by modulating endothelial cell attachment and migration.

Since many of DLC1's function is dependent on its RhoGAP activity, we examined whether the observed phenotypes in DLC2 knockdown HUVECs could be rescued by interrupting RhoA, the main target of DLC's RhoGAP. As shown in figure 5, treatment of siRNA against RhoA in the DLC2 knockdown HUVECs reversed the phenotypes in cell attachment, migration, and tube formation back to levels similar to those of control HUVECs, suggesting that DLC2 regulated these cellular processes through a RhoA dependent matter.

Discussion

By using the reporter-knockout approach, we have established the expression pattern of DLC2. Overall, DLC2 expression pattern is very similar to those of DLC1 and DLC3 (Durkin et al., 2007a; Durkin et al., 2002), although the levels are variable in some tissues. The similar expression patterns may explain the lack of developmental defects in DLC2 mutant mice due to compensation and/or functional redundancy. Our findings are overall in agreement with the recent report by Ng's group (Yau et al., 2009) that DLC2 is not required for mouse development and survival. However, although they reported that their DLC2-deficient mice were smaller and had less adipose tissue than the WT mice, we did not detect any difference in mouse body weight nor epididymal fat pad weight in our DLC2 KO mice (data not shown). In contrast to DLC2, lack of DLC1 leads to embryonic lethality with defects in the neural tube, brain, heart, and placenta (Durkin et al., 2005), indicating that DLC1 is not replaceable in embryogenesis. It will be interesting to investigate DLC3 knockout mice and double knockout among DLC family members to sort out their common and unique functions.

It is intriguing that matrigel was able to induce stronger angiogenesis in the DLC2 KO mice. Apparently, DLC2 KO endothelial cells were more sensitive to certain components within the matrigel, which is a solubilized basement membrane preparation extracted from the Engelbreth-Holm-Swarm (EHS) mouse sarcoma. The major components are laminin, collagen IV, heparin sulfate proteoglycan, and nidogen. In addition, trace amounts of TGFb (1.7 ng/ml), IGF-1 (5 ng/ml), EGF (0.5 ng/ml), NGF (<0.2 ng/ml), PDGF (<5 pg/ml), and

bFGF (<0.1 pg/ml) were detected in the growth factors reduced version of matrigel used in this study. Whether DLC2 KO endothelial cells are more sensitive to one or more of these factors or other unknown factors in the matrigel warrants further investigation. Consistent with the matrigel plug results, our B16 tumor cell xenograft studies also demonstrated that DLC2 KO endothelial cells responded better to factors produced by tumor cells than the WT cells did.

Reduced expression of DLC2 in breast, liver, lung, renal, colon, ovarian, uterine, and gastric cancers has been reported. In vitro data suggest that DLC2 suppresses tumor cell proliferation and colony formation in a RhoGAP dependent fashion (Ching et al., 2003; Leung et al., 2005). Together with its sequence homology to DLC1, DLC2 is proposed to function as a tumor suppressor. However, we did not observe spontaneous cancer development in DLC2 KO mice up to 20 months of age. Ng's group also showed that deficiency in DLC2 alone does not enhance hepatocarcinogenesis (Yau et al., 2009). It is very likely that it requires additional "hit(s)" for cancer formation. This is the case in DLC1, in which the lack of p53 and overexpression of c-myc in liver cells significantly promote tumor formation in the absence of DLC1 (Xue et al., 2008). It will be worthwhile to cross DLC2 KO mice with p53 null mice or other mouse cancer models to examine whether lack of DLC2 will enhance tumor progression in these mice. These studies are especially important since we have demonstrated a novel function of DLC2 in angiogenesis, which is an important process in growth and development, as well as in pathological processes. Tumor Angiogenesis is required for the non-invasive tumor to grow and for advanced tumor to spread (metastasis). In our case, dysregulated DLC2 is not directly associated with tumor cell proliferation, but allows endothelial cells responding more sensitive to certain factors released by tumor cells. Our B16 xenograft results demonstrated that loss of DLC2 enhances tumor angiogenesis and accelerates tumor development. Although the overall incidence of diethylnitrosamine-induced hepatocarcinogenesis was not increased in 35 weeks old DLC2 KO mice (Yau et al., 2009), it is possible that the effect of DLC2 deficiency is only critical at the early stage. It might be worthwhile to examine the diethylnitrosamine-treated mice at earlier time points. Interestingly, loss of DLC2 does not promote wound-induced angiogenesis in skin, indicating that DLC2 is not involved in all kinds of angiogenesis. In addition to cancer, angiogenesis also occurs in diabetic blindness, psoriasis, and rheumatoid arthritis. Whether DLC2 is participated in these diseases remains to be studied. Our studies suggest that the DLC2 KO mouse line may be a unique mouse model for disease-related angiogenesis studies.

Materials and Methods

Generation of DLC2 mice and genotyping

A DLC2 targeted ES cell clone was obtained from the Knockout Mouse Project Repository and injected into C57BL/6 blastocysts. The resulting male chimeras were mated with BALB/c females, and the DLC2 line was subsequently maintained on a C57BL/6 genetic background for five generations. Genotyping was performed by polymerase chain reaction (PCR) assay with primers specific for mouse DLC2 (a: F- ccacccagttggcatgagtc and b: R- tacaactactctgccaagtgc) and en2- β -geo (c: R- ccaactgacctggccaagaacat) to amplify a 1340-bp

fragment from the WT allele or a 351-bp fragment from the targeted allele. The PCR was performed at 94 °C for 5 min and followed by 30 cycles at 94 °C for 30s, 65 °C for 30s and 72 °C for 70s, 1 cycle at 72 °C for 7 min.

X-Gal staining

Mouse tissues were fixed in fixation buffer (0.2% glutaraldehyde in PBS plus 2 mM MgCl₂, 5 mM EGTA, and 0.02% NP-40, pH 7.3) at 4 °C for 4 h and embedded in OCT compound (Sakura). Frozen sections (10 μm) were re-fixed in fixation buffer at 4 °C for 10 min and washed three times in washing buffer (PBS plus 2 mM MgCl₂, 5 mM EGTA, 0.02% NP-40, and 0.01% Na-deoxycholate, pH 7.3) and stained at 37 °C for 6 h in the washing buffer with 1 mg/ml X-gal, 5 mM potassium ferricyanide, and 5 mM potassium ferrocyanide, and counterstained with nuclear fast red.

Immunohistochemistry

Frozen sections were fixed in cold acetone for 10 min. Endogenous peroxidase activity was blocked in 3% hydrogen peroxide in methanol for 30 min. Slides were incubated at 4 °C overnight with rat anti-mouse CD31 (PharMingen, San Jose, CA) at 1:200 dilution. Signal was detected with Vectastain ABC Elite Kit (Vector Laboratories, Burlingame, CA) and developed with diaminobenzidine substrate. Slides were counterstained with hematoxylin.

Matrigel plug assay

Growth factor-reduced matrigel (250 μl, BD Biosciences, San Jose, CA) containing 60 U/ml heparin (Sigma-Aldrich, St. Louis, MO) was subcutaneously injected into the mice (4–6 weeks old). After 4 days, matrigel plugs were harvested, photographed, and hemoglobin content was measured with Drabkin reagent (Ricca Chemical, Arlington, TX). Plugs were embedded in OCT and frozen sections were processed for immunohistochemical staining using CD31 antibody.

Mouse aortic ring assay

The mouse aortic ring assay was performed as described by Masson et al (Masson et al., 2005). Thoracic aortas were dissected and transferred to ice-cold DMEM. The fibroadipose tissues were removed and 1 mm long aortic rings were sectioned and embedded in growth factor-reduced matrigel within prepared cylindrical agarose wells. The aortic rings were cultured for two weeks and the outgrowth of endothelial tubes was counted.

Skin wound healing assay

Mice (12-week-old) were anesthetized and the surgical procedure was performed under aseptic conditions. Four full-thickness wounds were made on the backs of mice using a 2-mm skin punch (Acudern, Fort Lauderdale, FL). Seven days later, mice were euthanized and wounds were excised and embedded in OCT and frozen sections were processed for immunohistochemical staining using CD31 antibody as previously described. Photographs were taken and CD31 positive microvascular density were determined by Photoshop 7.0 (Adobe systems Inc., San Jose, CA) and ImageJ software (NIH).

Tumor xenograft assay

B16 murine melanoma tumor cells were injected (3×10^6 cells in 100 μ l of PBS) subcutaneously into the DLC2 KO and WT mice (4–6 weeks old). After 11 days, mice were sacrificed. Tumors were dissected, weighed and embedded. Microvascular density was assessed.

Wound healing migration assay

HUVECs were seeded on 6-well plates and cultured to confluence. The confluent monolayer was wounded with yellow tips and was allowed to migrate for 6 h. Photographs were taken and migration-distances were measured by ImageJ software (NIH).

Adhesion assay

HUVECs (1×10^4 /well) were seeded on 96-well plates pre-coated with 5 μ g/ml human plasma fibronectin and allowed to adhere for 30 min. Non-attached cells were removed and attached cells were stained and counted.

In vitro angiogenesis assay

HUVECs were seeded on a thin layer of growth factor-reduced matrigel at 10^4 cells/well of a 96-well plate in full culture medium and allowed to form a tubular structure for 6 h. The samples were examined and photographed. The photos were processed using ImageJ software (NIH).

Transfection of siRNA

Short interfering RNA against the human DLC2 (5'CACCUUCCAUCUCCUAAUTT), RhoA (GGCAGAGAU AUGGCAAACATT), and the universal negative control siRNA were used. The siRNAs were transfected into HUVECs by using Lipofectamine2000 (Invitrogen, Carlsbad, CA) per the manufacturer's protocol.

Antibody Production

Anti-DLC2 rabbit serum was raised against GST-DLC2 (154–395 aa) fusion protein. Anti-DLC2 antibodies were purified by affinity matrix using recombinant DLC2 (154–395aa) protein without the GST portion.

Acknowledgements

We thank the Knockout Mouse Project Repository for DLC2 ES cells. This work is supported by grants from the National Institutes of Health (CA102537) to SHL.

References

- Ching YP, Wong CM, Chan SF, Leung TH, Ng DC, Jin DY, Ng IO. Deleted in liver cancer (DLC) 2 encodes a RhoGAP protein with growth suppressor function and is underexpressed in hepatocellular carcinoma. *J Biol Chem.* 2003; 278:10824–30. [PubMed: 12531887]
- Durkin ME, Avner MR, Huh CG, Yuan BZ, Thorgeirsson SS, Popescu NC. DLC-1, a Rho GTPase-activating protein with tumor suppressor function, is essential for embryonic development. *FEBS Lett.* 2005; 579:1191–6. [PubMed: 15710412]

- Durkin ME, Ullmannova V, Guan M, Popescu NC. Deleted in liver cancer 3 (DLC-3), a novel Rho GTPase-activating protein, is downregulated in cancer and inhibits tumor cell growth. *Oncogene*. 2007a; 26:4580–9. [PubMed: 17297465]
- Durkin ME, Yuan BZ, Thorgeirsson SS, Popescu NC. Gene structure, tissue expression, and linkage mapping of the mouse DLC-1 gene (Arhgap7). *Gene*. 2002; 288:119–27. [PubMed: 12034501]
- Durkin ME, Yuan BZ, Zhou X, Zimonjic DB, Lowy DR, Thorgeirsson SS, Popescu NC. DLC-1: a Rho GTPase-activating protein and tumour suppressor. *J Cell Mol Med*. 2007b; 11:1185–207. [PubMed: 17979893]
- Leung TH, Ching YP, Yam JW, Wong CM, Yau TO, Jin DY, Ng IO. Deleted in liver cancer 2 (DLC2) suppresses cell transformation by means of inhibition of RhoA activity. *Proc Natl Acad Sci U S A*. 2005; 102:15207–12. [PubMed: 16217026]
- Liao YC, Lo SH. Deleted in liver cancer-1 (DLC-1): a tumor suppressor not just for liver. *Int J Biochem Cell Biol*. 2008; 40:843–7. [PubMed: 17521951]
- Liao YC, Shih YP, Lo SH. Mutations in the focal adhesion targeting region of deleted in liver cancer-1 attenuate their expression and function. *Cancer Res*. 2008; 68:7718–22. [PubMed: 18829524]
- Liao YC, Si L, Devere White RW, Lo SH. The phosphotyrosine-independent interaction of DLC-1 and the SH2 domain of cten regulates focal adhesion localization and growth suppression activity of DLC-1. *J Cell Biol*. 2007; 176:43–9. [PubMed: 17190795]
- Masson V, de la Ballina LR, Munaut C, Wielockx B, Jost M, Maillard C, Blacher S, Bajou K, Itoh T, Itohara S, Werb Z, Libert C, Foidart JM, Noel A. Contribution of host MMP-2 and MMP-9 to promote tumor vascularization and invasion of malignant keratinocytes. *Faseb J*. 2005; 19:234–6. [PubMed: 15550552]
- Qian X, Li G, Asmussen HK, Asnagli L, Vass WC, Braverman R, Yamada KM, Popescu NC, Papageorge AG, Lowy DR. Oncogenic inhibition by a deleted in liver cancer gene requires cooperation between tensin binding and Rho-specific GTPase-activating protein activities. *Proc Natl Acad Sci U S A*. 2007; 104:9012–7. [PubMed: 17517630]
- Testa G, Schaft J, van der Hoeven F, Glaser S, Anastassiadis K, Zhang Y, Hermann T, Stremmel W, Stewart AF. A reliable lacZ expression reporter cassette for multipurpose, knockout-first alleles. *Genesis*. 2004; 38:151–8. [PubMed: 15048813]
- Ullmannova V, Popescu NC. Expression profile of the tumor suppressor genes DLC-1 and DLC-2 in solid tumors. *Int J Oncol*. 2006; 29:1127–32. [PubMed: 17016643]
- Xiaorong L, Wei W, Liyuan Q, Kaiyan Y. Underexpression of deleted in liver cancer 2 (DLC2) is associated with overexpression of RhoA and poor prognosis in hepatocellular carcinoma. *BMC Cancer*. 2008; 8:205. [PubMed: 18651974]
- Xue W, Krasnitz A, Lucito R, Sordella R, Vanaelst L, Cordon-Cardo C, Singer S, Kuehnel F, Wigler M, Powers S, Zender L, Lowe SW. DLC1 is a chromosome 8p tumor suppressor whose loss promotes hepatocellular carcinoma. *Genes Dev*. 2008; 22:1439–44. [PubMed: 18519636]
- Yau TO, Leung TH, Lam S, Cheung OF, Tung EK, Khong PL, Lam A, Chung S, Ng IO. Deleted in liver cancer 2 (DLC2) was dispensable for development and its deficiency did not aggravate hepatocarcinogenesis. *PLoS One*. 2009; 4:e6566. [PubMed: 19668331]
- Yuan BZ, Miller MJ, Keck CL, Zimonjic DB, Thorgeirsson SS, Popescu NC. Cloning, characterization, and chromosomal localization of a gene frequently deleted in human liver cancer (DLC-1) homologous to rat RhoGAP. *Cancer Res*. 1998; 58:2196–9. [PubMed: 9605766]

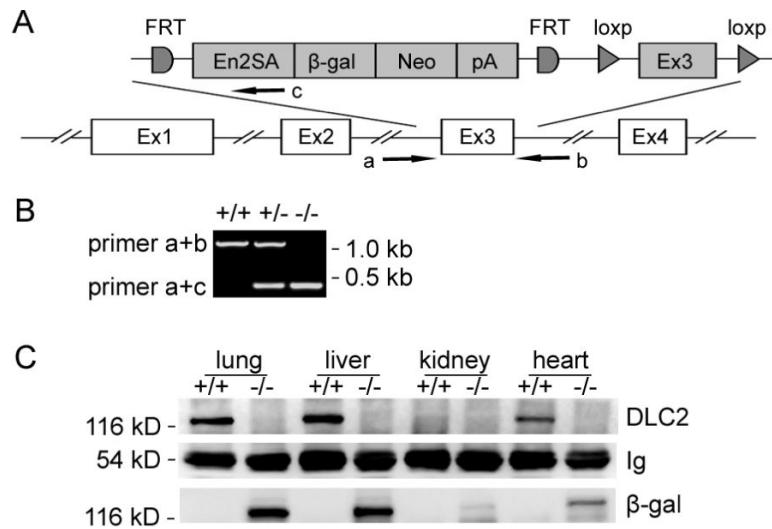


Figure 1. Generation of DLC2 reporter knockout mice

(A) Schematic diagram of targeting vector. (B) A representative genotyping by PCR analysis using primers specific for mouse DLC2 (a & b) and en2-β-geo (c). (C) Lung, liver, kidney and heart tissue lysates from wild-type (+/+) and homozygous (-/-) DLC2 mice were immunoprecipitated and immunoblotted with anti-DLC2 or anti-β-galactosidase to show that DLC2 protein expression was replaced by β-galactosidase in KO mice. Note that DLC2 is expressed at relatively low level in the wild-type kidney.

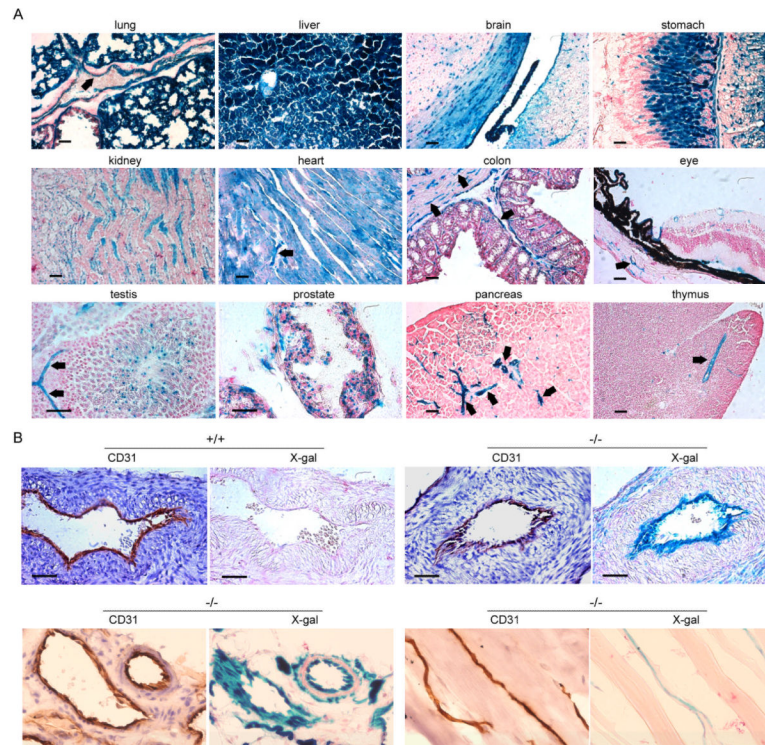


Figure 2. DLC2 expression pattern in mutant mice

(A) X-gal staining in 3-month-old DLC2 homozygous ($-/-$) mouse tissues. Arrows indicate blood vessels. Scale bar=50 μ m. (B) X-gal and CD31 immunohistochemical staining in consecutive sections of umbilical vessel (upper panel), stomach vessels (lower panel, left) and skeletal muscle (lower panel, right) showed that DLC2 co-expressed at CD31-positive endothelial cell layer and that blood vessels were histologically normal in DLC2 mutant mice. Scale bar=50 μ m.

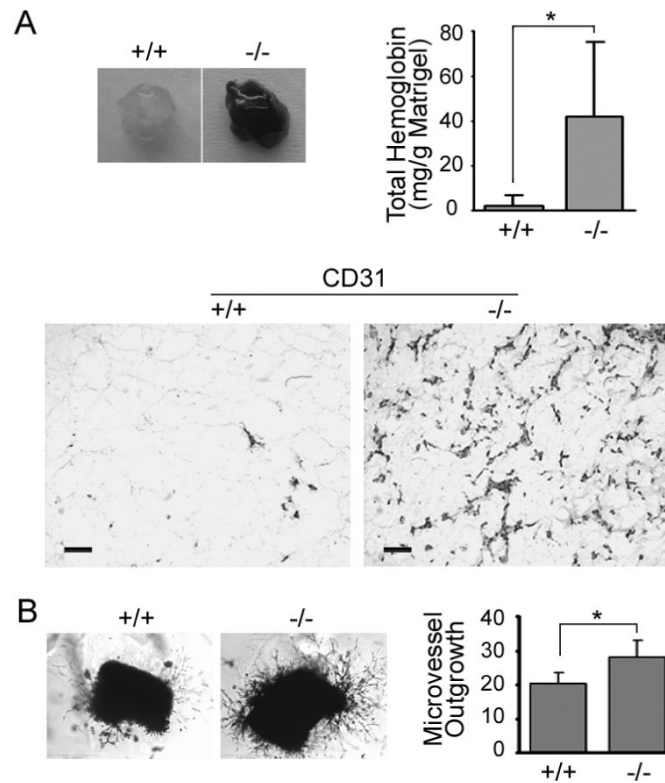


Figure 3. Loss of DLC2 enhances angiogenic responses induced by matrigel

(A) Angiogenic responses to matrigel plugs were more robust in DLC2 KO compared with the WT. The matrigel plug was bloodier in KO (left panel). Plugs from KO showed significant higher total hemoglobin contents (right panel) and more CD31-positive endothelial cells (lower panel) than WT samples. $*p < 0.05$ ($n = 6$). Scale bar = $50\mu\text{m}$. P-value was calculated by unpaired Student's t test. (B) Ex vivo sprouting of aortic explants from DLC2 KO is significantly enhanced. $*p < 0.05$ ($n = 5$). P-value was calculated by paired Student's t test.

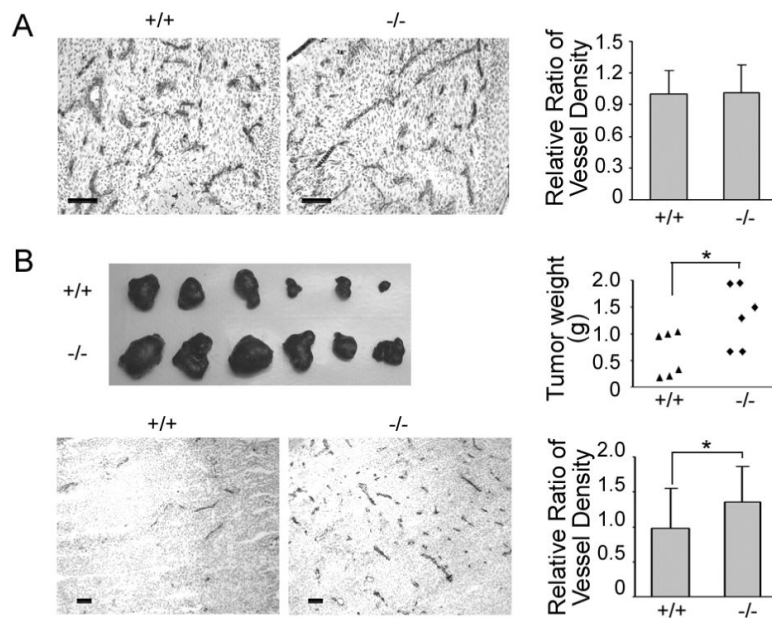


Figure 4. Lack of DLC2 enhances tumor development but not skin wound healing
 (A) Skin wound healing tissue showed no difference in microvascular densities between the DLC2 KO and WT mice. P-value was calculated by unpaired Student's t test. $P=0.93$ ($n=8$). Scale bar=50 μm . (B) Murine B16 tumor xenograft assays showed larger tumor sizes (upper panel) and higher microvascular densities (lower panel) in the DLC2 KO mice than WT mice. P-values were calculated by unpaired Student's t test. $*p<0.05$ ($n=6$). Scale bar=50 μm .

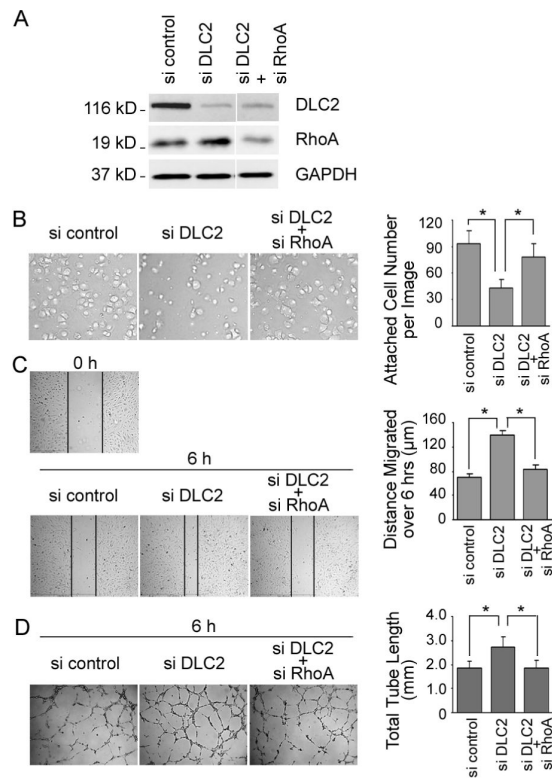


Figure 5. DLC2 regulates HUVEC attachment, migration, and tube formation in a RhoA dependent manner

HUVECs transfected with indicated siRNAs were used for immunoblotting analysis to confirm the knockdown efficiencies (A), cell attachment (B), wound healing migration (C), and in vitro angiogenesis assays (D). Representative images were shown. Each assay was independently performed three times. * $p < 0.05$. P-values were calculated by unpaired Student's t test.